

University of Szeged

Faculty of Pharmacy

**Institute of Pharmaceutical Technology and Regulatory Affairs**

Summary of the Ph.D. thesis

# **THE UTILIZATION OF TITANATE NANOTUBES AS DRUG DELIVERY SYSTEMS**

**Yasmin Ranjous**

Pharm.D., M.Sc.

**Supervisors:**

Dr. habil. Géza Regdon jr., PhD

and

Dr. habil. Tamás Sovány, PhD

Szeged

2021

University of Szeged

Graduate School of Pharmaceutical Sciences

Educational program: Pharmaceutical Technology  
Head: Prof. Dr. habil. Ildikó Csóka, PhD.

Institute of Pharmaceutical Technology and Regulatory Affairs  
Supervisors: Dr. habil. Géza Regdon jr. and Dr. habil. Tamás Sovány

**Yasmin Ranjous**

**The utilization of titanate nanotubes as drug delivery systems**

**Final Exam Committee:**

- Head:** *Prof. Dr. Piroska Révész, D.Sc.*, University of Szeged, Institute of Pharmaceutical Technology and Regulatory Affairs
- Members:** *Dr. Ildikó Bácskay*, Department of Pharmaceutical Technology, University of Debrecen.  
*Dr. habil. Aigner Zoltán*, University of Szeged, Institute of Pharmaceutical Technology and Regulatory Affairs

**Reviewer Committee:**

- Head:** *Prof. Dr. Loránd Kiss, DSc*, University of Szeged Faculty of Pharmacy, Institute of Pharmaceutical Chemistry
- Reviewers:** *Prof. Dr. Romána Zelkó, DSc*, Semmelweis University, University Pharmacy, Institute of Pharmaceutical Organization  
*Prof. Dr. Miklós Vecsernyés, DSc*, University of Debrecen Faculty of Pharmacy, Department of Pharmaceutical Technology
- Members:** *Dr. Attila Hunyadi, PhD*, University of Szeged Faculty of Pharmacy, Department of Pharmacognosy  
*Dr. Péter Doró, PhD*, University of Szeged Faculty of Pharmacy, Department of Clinical Pharmacy

Szeged

2021

## 1. INTRODUCTION

Conventional drug delivery systems may have limitations such as poor solubility, fluctuation in plasma concentration, patient non-compliance, concentration decrease at the site of action, and poor pharmacokinetics (PK). In contrast, nanotechnology-based drug delivery systems can help in delivering sparingly water-soluble drugs to their target location, achieving higher oral bioavailability and prolonging the drug blood circulation period. Furthermore, nanosized drugs may show better stability and, therefore, enhance the shelf life and acceptability of drugs by increasing either their uptake efficacy or patient compliance (1).

Metallic, organic, inorganic and polymeric nanostructures are often used as targeted drug delivery systems, particularly for poorly soluble and poorly permeable APIs. The biophysical and chemical characteristics such as shape and size have a significant influence on nanostructure efficacy (2). Nanotubes have a surface area five times higher than that of other NPs and an ideal inner diameter of 5–6 nm, which is suitable for loading even with large biological molecules. Furthermore, tubular NPs can be cell internalized in a higher percentage compared to their spherical counterparts (3).

The first nanotubes to be synthesized were carbon nanotubes (CNTs) in 1991 by Iijima, whereas titanate nanotubes (TNTs) were synthesized in 1996 by Hoyer. CNTs and TNTs display considerable similarities regarding their impressive mechanical, electrical, and optical properties. CNTs have promising results in drug delivery, but due to their high hydrophobicity, they accumulate in the human body, which leads to a risk of toxicity and carcinogenicity. Thus, CNTs are insoluble in aqueous solutions and cannot be used immediately in biomedical applications, whereas TNTs display strong hydrophilicity due to the capillary forces and their partially hydroxylated surface that can combine with hydrogen bonds causing outstanding wettability. Moreover, TNTs display excellent biocompatibility due to their good wettability and therefore improve cell adhesion. Based on the previously mentioned distinctive and promising characteristics of TNTs, we have selected them for further investigations (4).

## 2. AIMS

Tablets are the most common solid dosage form amongst marketed medicines, and they enhance patient compliance thanks to their wide-ranging advantages. However, it has been detected that 60–70% of the drug molecules are poorly water-soluble and/or poorly permeable, which leads to difficulties in their absorption from the GIT following oral administration. Many approaches were taken to overcome this challenge, such as crystalline solid formulations including salt formation and micronization of the crystalline compound, amorphous formulations including solid solutions and other formulation strategies, and lipid formation including solid dispersion. Nevertheless, these methods still face many obstacles, such as the unachievable salt formation of neutral compounds, the undesired particle size reduction of poorly wettable drugs, the uncertain physical stability of the product, potential drug or polymer crystallization, or low surfactant tolerance in chronic use (5). Therefore, poorly water-soluble and poorly permeable drugs still pose a major challenge to be manufactured as tablets.

TNTs have captivating characteristics, such as biocompatibility, hydrophilicity, surface chemistry, tunable geometries, and the ability to modify drug release kinetics. Furthermore, TNTs can load a higher amount of drug compared to CNTs and TNTs are superior to CNTs from the aspect of processability, biocompatibility and wettability (6).

For this purpose, our study was performed to demonstrate the importance of not only the optimized TNT-drug composites as an oral drug delivery system, but also their functionalization effect on enhancing the drug absorption from the GIT.

The main hypotheses of my research work were as follows:

- I. The optimization of the product quality of TNT-drug composites may be achieved by choosing a solvent with proper characteristics, e.g., dissolving ability, protic-aprotic nature and evaporation properties
- II. The functionalization of TNTs enables their hydrophobicity, to be tailored, thereby improving their permeability.
- III. Functionalization will not affect the toxicity profile of TNTs negatively.

### **3. MATERIALS**

#### **3.1. Hydrothermally synthesized titanate nanotubes and their composites**

TiO<sub>2</sub> and NaOH were used to prepare the hydrothermal TNTs. HCl 0.01 M was used to prepare TiHCl. Atenolol (ATN) (TEVA Pharmaceuticals PLC, Debrecen, Hungary), methanol (0.0168% water content) (Molar Chemicals Kft, Hungary) and 0.01 M aqueous solution of HCl (HCl 0.01 M) (Molar Chemicals Kft, Hungary) were applied to prepare TNT-ATN composites (TiATN). Hydrochlorothiazide (HCT) (TEVA Pharmaceuticals PLC, Debrecen, Hungary), 1 M aqueous solution of sodium hydroxide (NaOH 1M) (Molar Chemicals Kft, Hungary), DMF (0.012% water content) (Molar Chemicals Kft, Hungary), and DMSO (0.027% water content) (Molar Chemicals Kft, Hungary) were used for the synthesis of TNT-HCT (TiHCT).

#### **3.2. Functionalization**

Trichloro-octyl-silane (TCOS) (Sigma-Aldrich, St. Louis, Missouri, United States) and stearate (St) (VWR International, Radnor, PA, United States) were used to functionalize TNTs.

### **4. METHODS**

#### **4.1. Preparation of TNTs and their composites**

##### **4.1.1. Hydrothermal synthesis of TNTs**

###### **4.1.1.1. Pristine sodium trititanate (Na<sub>2</sub>Ti<sub>3</sub>O<sub>7</sub>) nanotubes (TNTs)**

NaOH was added to distilled water on a magnetic stirrer and then TiO<sub>2</sub> was added. The mixture was put in the autoclave inside a dry oven at 185 °C for 24 h and then cooled. After that, TNTs were washed with distilled water under vacuum and by using filter No#4.

###### **4.1.1.2. Hydrogen trititanate (H<sub>2</sub>Ti<sub>3</sub>O<sub>7</sub>) nanotubes (H-TNTs)**

TNTs were added to HCl 0.01 M in an ultrasonic bath. After that, HCl 0.01 M was added to the previous suspension on a magnetic stirrer and the mixture was dried in a dry oven for 24 h to remove the solvent.

###### **4.1.1.3. Magnesium trititanate (MgTi<sub>3</sub>O<sub>7</sub>) nanotubes (Mg-TNTs)**

Na-TNT was added to 0.1M MgCl<sub>2</sub> solution on a magnetic stirrer for 1 day. Then, the mixture was filtered by using glass filter No#4 under vacuum to obtain Mg-TNTs. This procedure was repeated three times to make sure that no Na-TNTs existed anymore. Finally, Mg-TNTs were washed with distilled water 8 times under vacuum and by using glass filter No#4.

## **4.1.2. Preparation of TNT-drug composites**

### **4.1.2.1. TiATN-Methanol/ TiATN-HCl/ TiHCT-DMF/ TiHCT-DMSO/ TiHCT-NaOH**

1:1 ratio of these composites were prepared by adding TNTs in the respective solvent in an ultrasonic bath, and ATN or HCT in the solvent on a magnetic stirrer. Then, the two prepared mixtures were added to each other on a magnetic stirrer until a homogenous mixture was obtained which was put in a vacuum distillation device to remove the solvent. However, HCl 37% was added to the final mixture of TiHCT-NaOH for neutralization and then was washed with distilled water in a vacuum dryer until pH = 9 to eliminate the solvent and was dried in a drying oven (Sanyo Electric Co., Ltd, Osaka, Japan).

## **4.2. Functionalization of TNTs**

### **4.2.1. TCOS-TNTs**

H-TNTs were added to toluene in ultrasonic bath for 1 h. After that, the suspension was heated to 80 °C in a condenser connected to nitrogen gas for 30 min. Then, TCOS reagent was added to the previous system in different concentrations, e.g. 1- 2- 10- 50- 100- 500- 1000 µl, covering the 0.001:1 - 2:1 molar ratios, respectively and mixed for one day. Finally, the functionalized TNTs were washed by hexane 8 times and dried in a drying oven at 80 °C.

### **4.2.2. MgSt- TNTs**

Mg-TNTs was added to distilled water in ultrasonic bath for 30 min. Following that, the mixture was heated to 80 °C in a magnetic stirrer and Na stearate VWR International was added in different (e.g. 0.001:1-0.1:1) molar ratios for 1 night. Finally, St-TNTs were filtered by using filter No#4 under vacuum and dried in a drying oven.

## **4.3. Morphology and size investigation**

Scanning electron microscope (SEM) (Hitachi 4700, Hitachi Ltd., Tokyo, Japan) and transmission electron microscope (TEM) (FEI Tecnai G2 20 X-TWIN, Hillsboro, OR, USA) were used to study the morphology and size of TNTs.

## **4.4. FT-IR spectrophotometer**

The interactions between the APIs and the TNTs were determined by using a Thermo Nicolet Avatar 330 FT-IR spectrometer (Thermo Fisher Scientific Ltd., Waltham, MA, USA).

#### **4.5. Surface free energy measurement**

The surface free energy was determined with a DataPhysics OCA20 (DataPhysics Instruments GmbH, Filderstadt, Germany) optical contact angle tester by using the sessile drop method.

#### **4.6. Thermoanalytical analysis**

A TGA/DSC1 simultaneous analyzer (Mettler-Toledo Ltd., Budapest, Hungary) was used to investigate the thermal behavior of TNTs, APIs, and composites. STARE Software (Mettler-Toledo Ltd, Budapest Hungary) was used to assess the curves.

#### **4.7. Drug release**

A DT700 (Erweka GmbH, Heusenstamm, Germany) dissolution tester was used to study drug release using the USP II method. A GENESYS 10S UV–VIS spectrophotometer (Thermo Fisher Scientific Ltd., Waltham, MA, USA) was used to measure the concentrations of the released drug which were assessed with Sigmaplot v12 (Systat Software Inc., San Jose, CA, USA) software.

#### **4.8. CHNS elemental analysis**

The content of carbon, hydrogen, nitrogen, and sulphur in organic materials was investigated rapidly by conducting CHNS elemental analysis. A Vario EL cube elemental analyzer (Elementar, Langenselbold, Germany) was used to analyze H, C, N, and S contents in the samples.

#### **4.9. Cytotoxicity and permeability detection**

Permeability and cytotoxicity experiments were tested on a Caco-2 human adenocarcinoma cell line in which energy dispersive X-ray fluorescent analyzer (Philips MiniPal PW 4025, Philips Analytical, the Netherlands) and MTT assay were used to measure the permeability and cytotoxicity, respectively.

## 5. RESULTS AND DISCUSSION

### 5.1. Optimization of the composite formation process and product quality

Based on the results of a previous study (7) the quality of TNT-drug composites is also related to the parameters of the chosen solvent. Thus, in our first hypothesis we have identified the protic-aprotic nature, the volatility, and the solubility of drugs as key factors of optimal solvent selection, in which we could achieve a strong interaction between the drug and the carrier.

#### 5.1.1. Properties of the TNT and TNT-HCl

The first step of our study was to test the reproducibility and robustness of the previously described synthesis method of TNTs (7) to ensure constant quality since the synthesis conditions affect strongly affect the dimensions and surface characteristics of TNTs.

The TEM images (Figure 1a) showed that the prepared TNTs have an average length of 116.22 nm (SD  $\pm$  49.49 nm) and an average diameter of 10.99 nm (SD  $\pm$  10.15 nm), which considerably approaches the previously described results of Sipos *et al.*

The SEM images (Figure 1b) displayed the characteristic aggregates of almost distinct and randomly oriented TNTs. Furthermore, there was no considerable difference in the surface characteristics of the new and the previous batch of TNTs according to the contact angle measurements (Table 1).

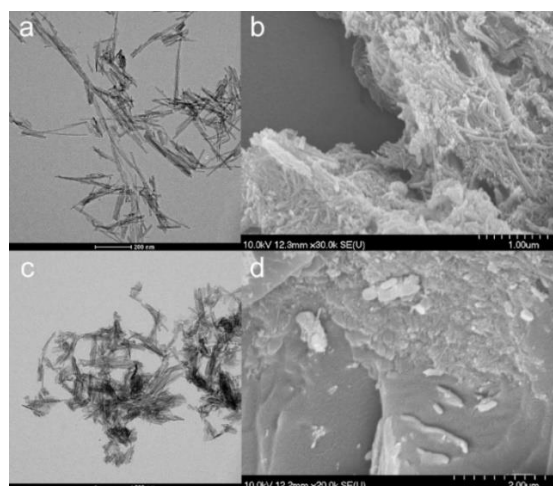


**Figure 1.** TEM (a,c) and SEM (b,d) micrographs of TNTs (a,b) and TNT–HCl 0.01 M (c,d) samples

**Table 1:** Surface free energy and polarity of TNTs, atenolol (ATN), hydrochlorothiazide (HCT), and their composites

Material	$\gamma_s$ (mJ/m <sup>2</sup> )	SD	$\gamma_s^{Disp}$ (mJ/m <sup>2</sup> )	SD	$\gamma_s^{Pol}$ (mJ/m <sup>2</sup> )	SD	Polarity%
TNTs (previous)	80.72	±0.64	43.78	±0.54	36.94	±0.35	45.76
TNTs (current)	80.85	±1.18	44.55	±0.53	36.31	±1.04	44.90
TNT-HCl	78.63	±2.07	43.10	±0.27	35.53	±2.05	45.19
ATN	59.48	±3.99	36.70	±2.96	22.77	±2.68	38.20
TiATN-ethanol	60.14	±4.25	40.45	±1.48	19.68	±3.87	32.72
TiATN-methanol	58.04	±2.01	37.12	±1.19	20.92	±1.47	36.04
TiATN-HCl	68.37	±2.26	34.83	±0.05	33.54	±2.26	49.06
HCT	69.51	±2.71	43.33	±0.79	26.18	±2.59	37.60
TiHCT-ethanol	78.25	±0.86	44.65	±0.57	33.60	±0.64	42.93
TiHCT-NaOH 1M	77.54	±1.89	44.52	±0.80	33.02	±1.71	42.59
TiHCT-DMF	71.47	±2.63	42.53	±0.29	28.94	±2.63	40.49
TiHCT-DMS	73.92	±1.42	45.29	±0.08	28.63	±1.42	38.72

The effect of diluted 0.01 M HCl on the properties of TNTs was tested by preparing TNT–HCl samples as a reference (Figure 1c, d). The TEM images showed a slight decrease in the dimensions of TNT-HCl compared to native TNTs, with an average length of 83.92 nm (SD ± 42.48 nm) and an average diameter of 8.78 nm (SD ± 1.76 nm). Nevertheless, neither the surface characteristics (Table 1) nor the FT-IR spectrum (Fig. 2) displayed a considerable difference from the results of native TNTs. Therefore, no noteworthy difference was expected in the behavior of TNT and TNT–HCl from the aspect of composite formation ability.

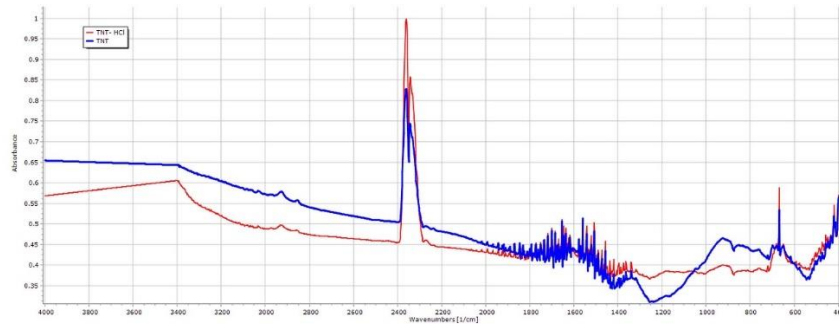


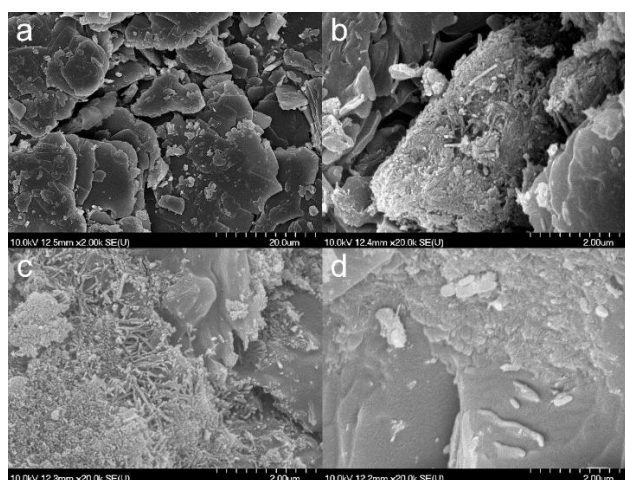
**Figure 2.** FT-IR spectra of TNTs and TNT–HCl 0.01 M

### 5.1.2. Effect of various solvents on composite formation with ATN

In the previous study of (7) it was confirmed that composite formation was insufficient for TiATN-ethanol (Fig. 3b) since both the aggregates of TNTs and the smooth surfaced particles of crystalline ATN (Fig. 3a) were clearly visible in the SEM images. A stronger interaction but still insufficient composite formation was observed in the TiATN-methanol sample (Fig. 3c).

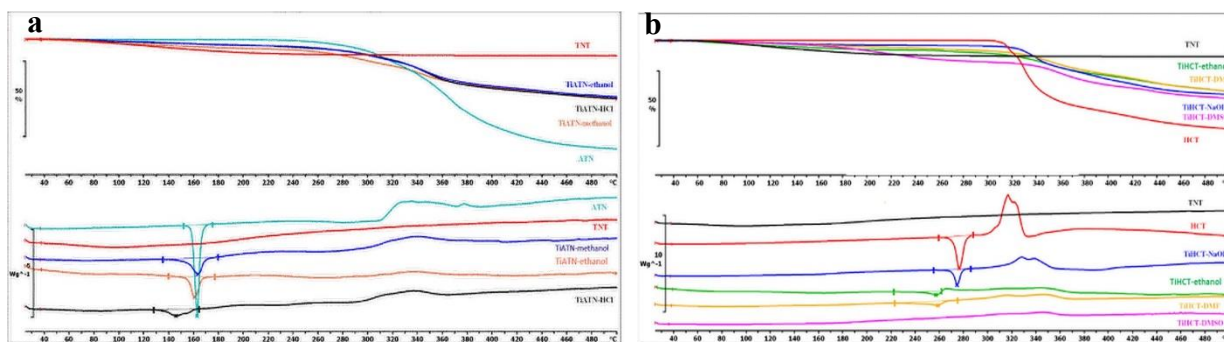
Interestingly, a rough surface and highly ordered aggregations were detected in TiATN-HCl which indicates a more adequate composite formation (Fig. 3d).

The OCA measurement (Table 1) showed that the  $\gamma_s$  for TiATN-ethanol, TiATN-methanol and ATN were almost identical to each other, which may indicate not pure TNTs but TNT-ATN composites aggregated to the surface of bigger ATN particles. In contrast, distinctly different values of  $\gamma_s$  and polarity for TiATN-HCl were detected, which may reflect not only a kind of interaction between  $\text{NH}_3^+$  from ATN and the hydrophilic sites in TNTs enriching the hydrophobic regions in TNTs, but also a different particle forming mechanism than in the case of other solvents, which leads to a different expected behavior during processing and use.



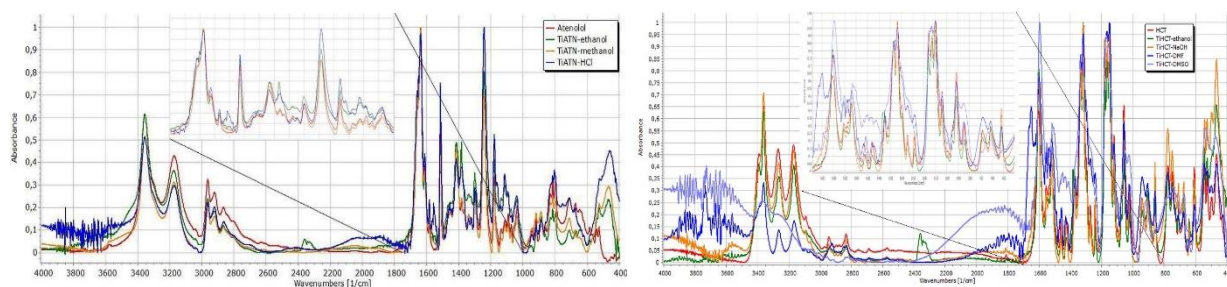
**Figure 3.** SEM micrographs of atenolol (a), TiATN-ethanol (b), TiATN-methanol (c), and TiATN-HCl 0.01 M (d)

Fig. 4a displays that the DSC curve of ATN contains an endothermic and a broad exothermic peak. The sharp endothermic peak at 155.21 °C represents the fusion of the compound and the exothermic peak describes its decomposition, which is supported by the TG curve of ATN. The enthalpy of fusion for this peak in TiATN-ethanol and TiATN-methanol was declined which may indicate the poor composite formation. On the other hand, a significant decrease in the fusion enthalpy to  $-40.55 \text{ Jg}^{-1}$  were detected in the TiATN-HCl composite, which may be resulted due to the stronger interactions and the considerable particle size reduction of ATN.



**Figure 4.** DSC and TG curves of TNT, ATN, TiATN-methanol, TiATN-ethanol and TiATN-HCl (a) and TNT, HCT, TiHCT-ethanol, TiHCT-NaOH, TiHCT-DMF and TiHCT-DMSO (b)

These results were supported by the FT-IR spectra, which displayed no substantial differences between the spectra of ATN, TiATN-ethanol and TiATN-methanol (Fig. 5). On the other hand, changes in the TiATN-HCl spectrum were observed, namely the appearance of a new peak at  $1560\text{ cm}^{-1}$ , indicating the protonation of the carbonamide group and wide low intensity peaks between  $1900\text{--}2100\text{ cm}^{-1}$  and  $2300\text{--}2500\text{ cm}^{-1}$ , indicating the protonation of the secondary amino group.



**Figure 5.** FT-IR spectra of ATN and its composites (a) and HCT and its composites (b)

However, the strongest reaction between TNTs and ATN was achieved by using HCl 0.01 M as a solvent in spite of the slow evaporation rate, which can be explained by the protonation of the carboxyl amide and secondary amino groups of ATN, resulting in repulsion between ATN molecules and in a possible increase in their H-bonding strength in the presence of polyfunctional carriers as TNTs. These effects also cause characteristic ATN-TNT interactions, which result in an increased dissolution rate from the composites due the formation of stable nanocrystals on the surface of the carrier (Fig. 6a).

In conclusion, ATN shows good solubility in 70 w/w% ethanol solution, methanol and HCl 0.01M. The Janus-faced properties of the TiATN-ethanol sample can be explained by the fast supersaturation of the solution resulting from the fast evaporation of the ethanol content

followed by the slower speed of water removal, which induced the concentration of ATN molecules and promoted the formation of ATN-ATN bonds instead of ATN-TNT ones. This latter effect was not observed during the fast removal of water-free methanol, whereas the repulsive effect between protonated ATN molecules prohibited the formation of ATN-ATN interactions despite the slower solvent removal speed in 0.01 M HCl solution.

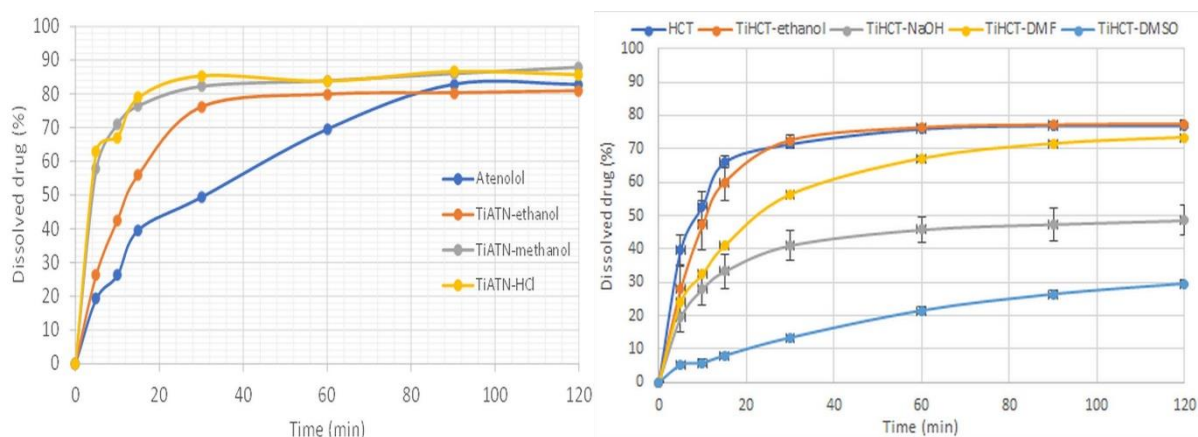


**Figure 6.** Dissolution study of TiATN (a) and TiHCT (b) composites in gastric juice (non-sink conditions)

### 5.1.3. Effect of various solvents on composite formation with HCT

The SEM micrographs display the strong recrystallization of HCT (Fig. 7a) from ethanol and NaOH (Fig. 7b,c) with the appearance of HCT crystals covered by the composites. On the other hand, no considerable recrystallization was observed in TiHCT-DMF and TiHCT-DMSO (Fig. 7d,e), and only strong compacts of TNTs with increased thickness are visible, which suggests an appropriate loading of the nanotubes with the API, which was also supported by the results of the OCA measurements (Table 1) and DSC analysis.

The OCA results showed that  $\gamma_s$  and polarity values for TiHCT-ethanol and TiHCT-NaOH were higher compared to HCT due to the accumulation of TNTs on the surface of HCT crystals. In contrast, TiHCT-DMF and TiHCT-DMSO revealed  $\gamma_s$  values similar to HCT due to the surface coverage of TNTs with HCT molecules.

The DSC curve (Fig. 4b) of HCT shows that the fusion of the API could be recognized near 270.67 °C, which was followed by a characteristic exothermic event near 320 °C, ascribed to the decomposition of the material. The TiHCT-NaOH composite exhibited a slight shift in the melting peak which indicates poor composite formation and this can be explained by the long evaporation time.

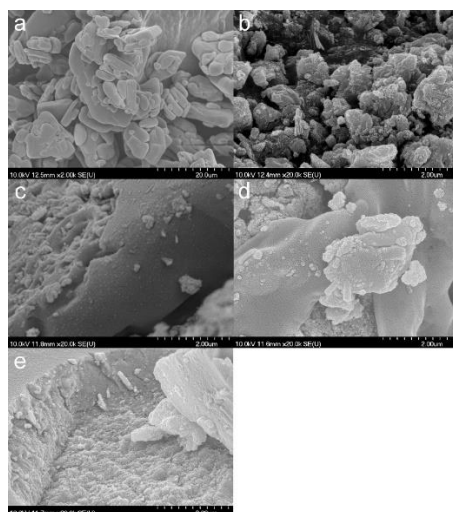


**Figure 7.** SEM micrographs of HCT (a), TiHCT-ethanol (b), TiHCT-NaOH (c), TiHCT-DMF (d), TiHCT-DMSO (e)

TiHCT-ethanol and TiHCT-DMF revealed a higher shift in the melting peak which indicates a stronger interaction. Nevertheless, an improved composite formation was observed in DMF, but interestingly, no fusion peak can be seen in the case of TiHCT-DMSO composites, which can be explained by the formation of amorphous HCT particles instead of nanocrystals. All those findings were in accordance with the results of the XRPD results (Fig. 8).

The X-ray diffractogram of TiHCT-DMSO shows only the characteristic peaks of the crystalline TNTs, which clearly shows HCT bonding with TNTs in an amorphous form, which is highly expected to ensure an improved dissolution rate, whereas the other composites contained HCT in a (nano)crystalline form. However, a new polymorphic form of HCT was recrystallized from DMF (the metastable Form II or DMF solvate instead of the starting stable Form I) (8).

The FT-IR spectra were normalized to the peak at  $1319\text{ cm}^{-1}$  (Fig. 5b). The peaks at  $3391\text{ cm}^{-1}$  shows non-associated NH stretching, and the right shift of this peak at  $3269\text{ cm}^{-1}$  indicates the increasing strength of interactions in TiHCT composites in ethanol, NaOH, DMF, DMSO, respectively. The merging of these peaks in DMSO suggests a very strong association, which may also be due to the amorphous state of the drug in the composite.

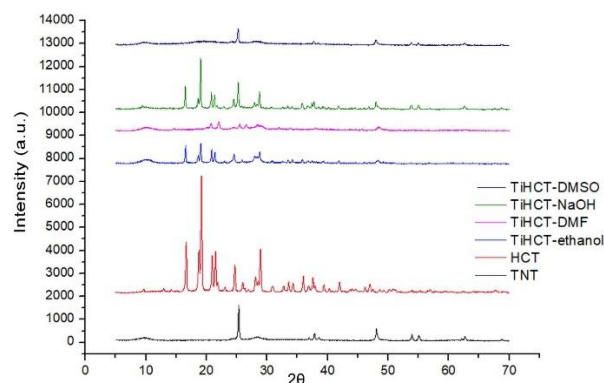


**Figure 8.** XRPD spectra of HCT and its composites

The strength of interactions fundamentally determines the dissolution rate of the drug from the composites (Fig. 6b). There was no considerable difference in the dissolution rates of pure HCT and TiHCT-ethanol composite, in which the weakest interaction was observed. The increasing strength of the interactions resulted in a controlled dissolution rate and led to the switch of release kinetics from first order to power law model described by Korsmeyer and Peppas. TiHCT-DMSO exhibited the most considerable elongation of drug release. It is well visible that the decrease in the release rate of TiHCT-NaOH was higher than expected, which may be due to the large size of the HCT particles due to the slow recrystallization of the drug from the solvent.

In conclusion, HCT was dissolved in 70 w/w% ethanol solution and NaOH 1 M as an analog of the experiments with ATN. DMF and DMSO were successful in forming the TiHCT composites since H-bonding was featured between HCT and TNTs due to the lack of drug-solvent interactions. Nevertheless, despite the stabilized nanocrystalline form or HCT “recrystallizing” from DMSO in an amorphous form, an extended release of HCT from the composites was noted due to the very strong drug-carrier interactions.

Overall, the assumptions of the first hypothesis were confirmed as protic-aprotic nature, solvent volatility and drug solubility play key roles in the composite formation process. The formation of strong TNT-API composites may be achieved optimally by choosing a highly volatile aprotic solvent. Nevertheless, the use of protic solvents should be considered if the drug is protonable. However, the high strength of drug-carrier interactions may influence drug detachment, and thus the final product characteristics, including release rate and behaviour in biological environment. The strength of interactions may be optimized by tailoring the surface characteristics of TNTs by functional modifications.

## 5.2. The functionalization of TNTs

In the present part of the study, TCOS and MgSt were selected to functionalize the TNTs, to prove that the functionalization of hydrophilic TNTs with hydrophobic materials is a good technique to enhance their absorption into the systemic circulation.

### 5.2.1. Physical properties of the functionalized TNTs

Pristine Na-TNTs (Fig 9a) have a considerably elongated structure with an external diameter of 8-12 nm, and highly variable length (100-1000 nm). H-TNTs (Fig 9b) show identical physical dimensions but have an increased aggregation tendency due to the decreasing electrostatic repulsion resulting from the removal of  $\text{Na}^+$  ions. Mg-TNTs (Fig. 9c) have the same diameter of 8-12 nm but the mechanical agitation during the ion-exchange procedure resulted in considerable fragmentation, so the length of the nanotubes varies mostly in the 100-300 nm range. Similar fragmentation of the longer nanotubes was observed in the case of the functionalized samples (Fig. 9d-g) along with a slight increment of the diameter, which depends on the amount and orientation of the functionalizing agent on the surface of TNTs. Nevertheless, all samples have a strongly elongated tubular structure with an aspect ratio  $>10$ .

The OCA measurement showed a gradual increment in optical contact angle with the increasing concentration of TCOS and complete surface coverage was achieved by the application of 100  $\mu\text{L}$  reagent volume (e.g. 0.2:1 molar ratio). These results were supported by the CHNS elemental analysis, which displayed a continuous augmentation in carbon percentage with the increasing amount of functionalizing TCOS (Fig.10).

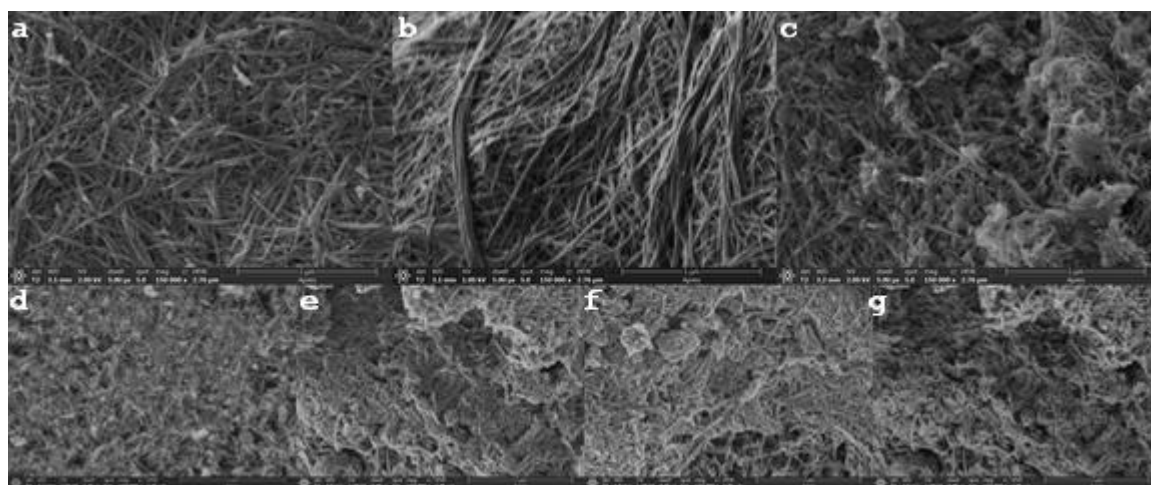


**Figure 9.** SEM of Na-TNT (a), H-TNT (b), Mg-TNT (c), TCOS-TNT 10 (d), TCOS-TNT 50 (e), St-TNT (0,05:1) (f) and St-TNT (0.1:1) (g) samples with 150.000x magnification

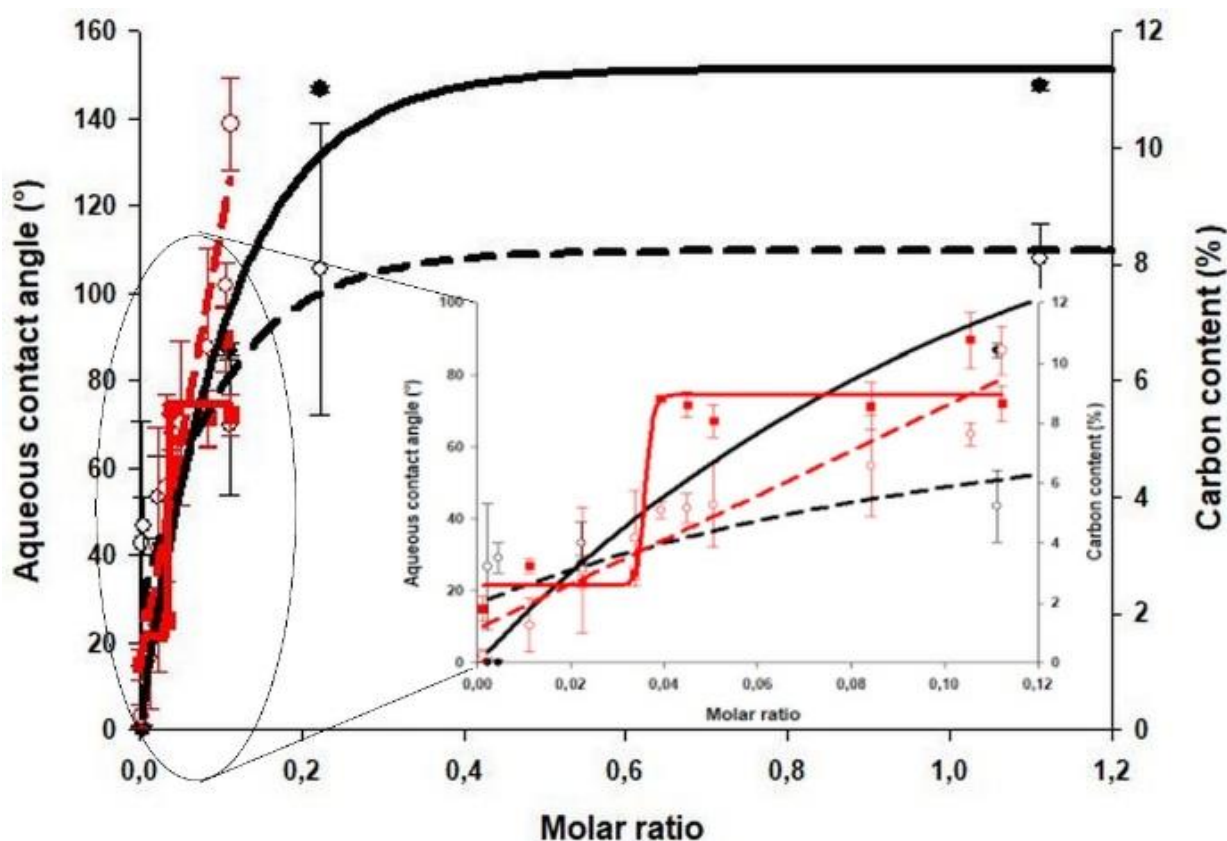


**Figure 10.** The aqueous contact angles (CA) and carbon percentage (C%) of TCOS-TNTs and St-TNTs at different reagent concentrations (CA of TCOS-TNT (black line); C% of TCOS-TNT (black dashed line), CA of St-TNT (red line), C% of St-TNT (red dashed line)

In contrast, the OCA measurement revealed that low concentrations of St could just slightly increase OCA of Mg-TNTs, but after exceeding of a certain threshold around 0.035:1 ratio and despite the linear increment of the carbon content, the surface turned from hydrophilic to hydrophobic (Fig. 10). A possible explanation that above this threshold the St molecules are oriented differently on the surface of TNTs, prohibiting the access of water to the sample. After that only a slight increment could be detected until it stabilizes between 80-90°, but it should be noted, that the maximum aqueous contact angle is considerably smaller as in the case of TOCS-TNTs. Less St coverage resulted in getting a hydrophobic surface that may bear an advantage of keeping more binding sites for the drugs which may lead to a higher possible drug load in this system.

### 5.2.2. Toxicity and permeability of functionalized TNTs

In a previous study (9), no detectable cytotoxicity of Na-TNTs was observed up to a concentration of 5 mg/mL, but in the current study a considerable decrease in cell viability was observed if Mg-TNTs were applied in this concentration (Fig. 11).

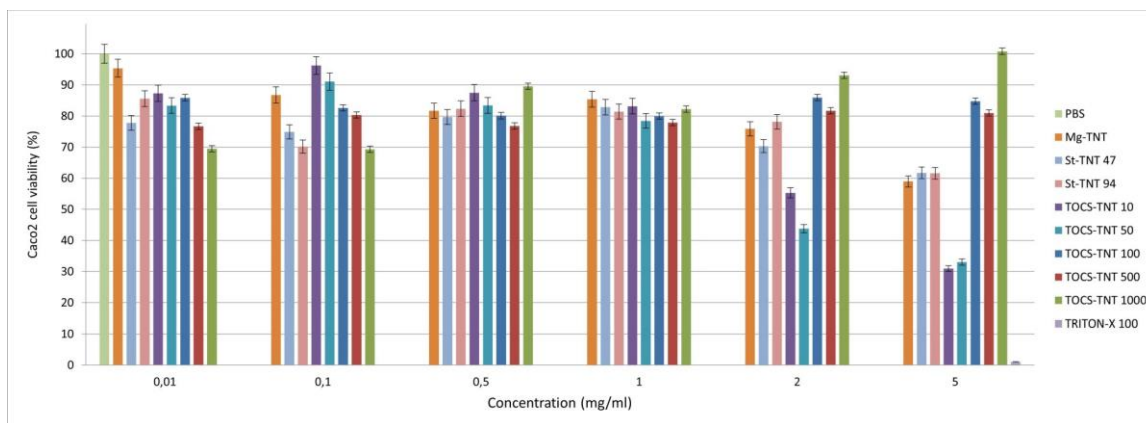


**Figure 11.** The viability assays of Caco-2 cells after being exposed to functionalized TNTs

This may indicate that the replacement of  $\text{Na}^+$  to  $\text{Mg}^{2+}$  ions on the surface of TNTs also has negative influence on cell interactions, but based on the MTT cytotoxicity test, it is still considered as non-cytotoxic in the concentration range of 0,01-2 mg/mL. In addition, considerable differences were observed in the toxicity of various functionalized TNTs, especially at higher concentrations.

The toxicity results displayed a considerable decrease in cell viability in for TCOS-TNT 10- and 50-  $\mu\text{L}$  samples, possibly due the use of H-TNT as a starting material. On the other hand, the lower toxicity presented by MgSt-TNTs which was similar to Mg-TNTs, indicates that the effect may be connected to the presence of  $\text{Mg}^{2+}$  ions and not to St molecules.

### 5.2.3. Permeability results

During the permeability test the highest safe concentration (1 mg/mL) was applied to achieve a higher maximum drug-dose during further utilization. The transepithelial electrical resistance (TEER) of the cells before TNT exposure was  $602 \pm 116 \Omega/\text{cm}^2$ . For Caco-2 cells, this value may vary in a very large range ( $200\text{-}2400 \Omega/\text{cm}^2$ ) (10), the obtained results indicate an intact cell layer. Nevertheless, a considerable decrease ( $22.1 \pm 16.7\%$ ,  $12.4 \pm 11.1\%$ ,  $37.1 \pm 8.4\%$  and  $23.6 \pm 17.4\%$  for TCOS-TNT 10, TCOS-TNT 50, St-TNT (0.05:1), and St-TNT (0.1:1) samples, respectively in the TEER values was observed after exposure to TNTs, which indicates the perturbation of the integrity of the cell membrane or tight-junctions. However, microscopic investigation showed no change in the cell morphology or layer-integrity, before and after the test, which may indicate a periodic distortion of the membrane integrity by the penetrating nanotubes. Nevertheless, the relative change of various samples showed partial correlation with the results of the permeability tests (Table 2), which revealed that the aqueous contact angle (CA) values should be between  $60\text{-}90^\circ$  to achieve appropriate absorption, while the cell

integrity was exhibited the smallest distortion for samples between 80-90°CA. Below 40° the surface is too hydrophilic to achieve passive transportation through the cell membrane, while in the 40-60° range the samples may be absorbed considerably slower than the ones with 60-90° CA, and causes higher distortions in cell integrity, possibly due to the higher hydrophilicity.

In a previous study (9) no detectable number of pristine Na-TNTs have been found on the basolateral side of the cell monolayer, indicating that the intestinal cell layer is impermeable to this material, possibly due to its high hydrophilicity. In contrast, present study revealed that functionalized samples exhibited considerable permeability through the cell monolayer (Table 2). According to the results, the penetration of samples with small (30°) CA is hindered as more than 40% of the originally inserted value was still detected on the apical side. The best permeability rate was observed for samples with 70-90° CA, where the amount permeated to the basolateral side was increased with the increasing CA. In case of sample TCOS-TNT 100 where the CA was around 140° no detectable amount was measured both in apical and basal compartment. A possible explanation that due to the inappropriate wetting and dispersion, the TNTs were sedimented and adhered to the cell layer without visible absorption through the membranes or were completely accumulated in the cells, which would bear a potential risk of toxicity. Nevertheless, in both cases the sample is inappropriate for the planned application.

**Table 2:** Results of the permeability tests

Material	Aqueous CA (°)	Apical amount (%)	Basal amount (%)
TCOS-TNT 10	27.70±2.10	40.94±10.49	8.47±0.30
TCOS-TNT 50	86.66±1.90	27.94±14.83	8.39±0.24
TCOS-TNT 100	146.65±0.60	n.m	n.m
St-TNT 47	71.75±3.58	26.98± 6.66	8.75±0.78
St-TNT 94	89.55±7.66	27.16±11.13	11.49±0.67

This part of the experimental work emphasized the importance of functionalizing the TNTs to improve their absorption after the oral administration. We have confirmed the second hypothesis, according to which increasing the hydrophobicity of TNTs may increase the cell permeability. Nevertheless, the validity of the third hypothesis, namely that the increased hydrophobicity may not affect the toxicity, should be partially reconsidered, since the functionalized samples exhibited slightly increased toxicity, but it was connected to the altered surface charge due to ion exchange during the functionalization procedure.

## 6. CONCLUSIONS AND PRACTICAL USEFULNESS

In this study, TNT composites with ATN and HCT were prepared to improve the drug dissolution profile from the composites in which ATN and HCT were chosen as model drugs from the third and fourth classes of BCS.

- I. Choosing the appropriate solvent is essential from the aspect of composite formation efficacy. Solvent volatility is important, but its protic/aprotic nature depends on the drug properties, with protic solvents being preferable for protonable drugs, otherwise aprotic solvents are more advantageous.
- II. The extent of the strength of interaction between TNTs and drugs directly affects drug detachment inside the human body, thus it should be estimated based on the administered oral dosage form, in which weak interaction is enough in immediate release drugs and strong interaction is favored for extended-release purposes.

TNTs were functionalized to obtain increased hydrophobicity and enhance their absorption from the GIT, with two different methods were compared to each other. For this purpose, TCOS and St were used in different concentrations with a view to optimizing the functionalization method and determining the optimal functionalization percentage.

- I. The functionalization of TNTs is crucial to enhance their hydrophobicity and therefore their permeability and may strengthen the interaction between TNTs and drugs.
- II. The toxicity of functionalized TNTs has to be checked due to the changed surface charge.

**The practical relevance and new approaches of this research work are the following**

- I. Our hypothesis of choosing the optimal solvent proved to be a promising approach for enhancing the solubility of poorly water-soluble drugs.
- II. Functionalized TNTs are potential drug carriers for the oral administration route since they display good permeability and toxicity profiles.

## REFERENCES

1. Suri SS, Fenniri H, Singh B. Nanotechnology-based drug delivery systems, *J. Occup. Med.* 2, 16 (2007).
2. Mirza AZ, Siddiqui FA. Nanomedicine and drug delivery: a mini review, *Int. Nano Lett.* 4, 94 (2014).
3. Kulkarni HP. Synthesis and applications of titania nanotubes, Drug delivery and ionomer composites: The University of North Carolina at Chapel Hill. (2008).
4. Ranjous Y, Regdon jr G, Pintye-Hódi K, Sovány T. Standpoint on the priority of TNTs and CNTs as targeted drug delivery systems, *Drug Discov. Today.* 24, 1704-1709 (2019).
5. Patel BD, Modi RV, Thakkar NA, Patel AA, Thakkar PH. Development and characterization of solid lipid nanoparticles for enhancement of oral bioavailability of Raloxifene, *J. Pharm. Bioallied Sci.* 4(Suppl 1), S14 (2012).
6. Wang Q, Huang JY, Li HQ, Zhao AZ, Wang Y, Zhang KQ, Sun HT, Lai YK. Recent advances on smart TiO<sub>2</sub> nanotube platforms for sustainable drug delivery applications, *Int. J. Nanomedicine.* 12, 151 (2017).
7. Sipos B, Pintye-Hódi K, Kónya Z, Kelemen A, Regdon jr G, Sovány T. Physicochemical characterisation and investigation of the bonding mechanisms of API-titanate nanotube composites as new drug carrier systems, *Int. J. Pharm.* 518, 119-129 (2017).
8. Saini A, Chadha R, Gupta A, Singh P, Bhandari S, Khullar S, Mandal S, Jain DS. New conformational polymorph of hydrochlorothiazide with improved solubility, *Pharm Dev Technol.* 21, 611-618 (2016).
9. Fenyvesi F, Kónya Z, Rázga Z, Vecsernyés M, Kása P, Pintye-Hódi K, Bácskay I. Investigation of the cytotoxic effects of titanate nanotubes on Caco-2 cells, *AAPS PharmSciTech.* 15, 858-861 (2014).
10. Srinivasan B, Kolli AR, Esch MB, Abaci HE, Shuler ML, Hickman JJ. TEER measurement techniques for in vitro barrier model systems, *J. Lab. Autom.* 20, 107–126 (2015).

## LIST OF ORIGINAL PUBLICATIONS

1. **Ranjous, Y.**, Regdon jr., G., Pintye-Hódi, K., & Sovány, T. (2019). Standpoint on the priority of TNTs and CNTs as targeted drug delivery systems, *Drug Discovery Today*. 24(9), 1704-1709 (2019).

**IF: 6.800**

2. **Ranjous, Y.**, Regdon jr., G., Pintye-Hódi, K., Varga, T., Szenti, I., Kónya, Z., & Sovány, T. Optimization of the production process and product quality of titanate nanotube–drug composites, *Nanomaterials* 9(10), 1406 (2019).

**IF: 4.324**

3. **Ranjous, Y.**, Kósa, D., Ujhelyi, Z., Regdon jr., G., Szenti, I., Nagy, KA., Kónya, Z., Bácskay, I., & Sovány, T. Toxicity and permeability investigation of functionalized titanate nanotubes on Caco-2 cell line, *Acta Pharmaceutica Hungarica* 91, 31-39 (2021).

## PRESENTATIONS RELATED TO THE THESIS

### Verbal presentations:

1. **Yasmin Ranjous**, Géza Regdon jr., Tamás Sovány: Formulating different TNT-API composites as (targeted) drug delivery systems. I. Symposium of Young Researchers on Pharmaceutical Technology, Biotechnology and Regulatory Science. January 31, 2019. Szeged, Hungary.
2. **Yasmin Ranjous**, Géza Regdon jr., Tamás Sovány: Investigation the effect of solvent selection on the production process and product quality of titanate nanotube-drug composites. II Fiatal Technológusok Fóruma. April 10, 2019. Budapest, Hungary.
3. **Yasmin Ranjous**, Géza Regdon jr., Tamás Sovány: The role of solvents in enhancing the production process of titanate nanotube-drug composites. Towards a Knowledge Economy for Postwar Syria, The Role of Syrian Researchers at Home and Expatriate. August 7-8, 2019. Damascus, Syria.
4. Sovány Tamás, **Yasmin Ranjous**, Sipos Barbara, Hódi Klára, Kónya Zoltán, ifj. Regdon Géza: Titanát nanocső-hatóanyag kompozitok előállításának optimalizálása. Gyógyszer technológiai és Ipari Gyógyszerészeti Konferencia. September 26-28, 2019. Siófok, Hungary.

5. **Yasmin Ranjous**, Géza Regdon jr., Tamás Sovány: The prominence of titanate nanotubes' functionalization on their physicochemical properties and biological applications as drug delivery system. II. Symposium of Young Researchers on Pharmaceutical Technology, Biotechnology and Regulatory Science. January 23-24, 2020. Szeged, Hungary.
6. **Yasmin Ranjous**, Géza Regdon jr., Zoltán Kónya, Tamás Sovány: Investigation of physical properties, toxicity and permeability of functionalized titanate nanotubes as novel vectors for drug delivery. EUGLOH Annual Student Research Conference. September 28-30, 2020. Online conference.
7. **Yasmin Ranjous**, Dóra Kósa, Zoltán Ujhelyi, Krisztina Anita Nagy, Zoltán Kónya, Ildikó Bácskay, Géza Regdon jr., Tamás Sovány: The use of functionalized titanate nanotubes as drug delivery systems. III Fialat Technológusok Fóruma. December 14, 2020. Online conference.
8. **Yasmin Ranjous**, Dóra Kósa, Zoltán Ujhelyi, Géza Regdon jr., Krisztina Anita Nagy, Zoltán Kónya, Ildikó Bácskay, Tamás Sovány: Optimization of the functionalization method of titanate nanotubes in order to use them as drug delivery systems. III Symposium of Young Researchers on Pharmaceutical Technology, Biotechnology and Regulatory Science. January 20-22, 2021. Online conference.

**Poster presentations:**

9. **Yasmin Ranjous**, Géza Regdon jr., Zoltán Kónya, Tamás Sovány: Optimization of the production process and product quality of titanate nanotube–drug composites. 12<sup>th</sup> Central European Symposium on Pharmaceutical Technology and Regulatory Affairs. September 20-22, 2018. Szeged, Hungary.

**PRESENTATIONS NOT RELATED TO THE THESIS**

1. **Yasmin Ranjous**, Géza Regdon jr., Tamás Sovány, Jamelah Hasian: Improvement of Gabapentin's Stability by Using Different Excipients and Varying the Ambient Conditions. EUFEPS Annual Meeting. May 24-26, 2018. Athens, Greece.